

# Loss of $\beta$ Pix Causes Defects in Early Embryonic Development, and Cell Spreading and Platelet-Derived Growth Factor-Induced Chemotaxis in Mouse Embryonic Fibroblasts

TaeIn Kang<sup>1,3</sup>, Seung Joon Lee<sup>2,3</sup>, Younghee Kwon<sup>1,3</sup>, and Dongeun Park<sup>1,\*</sup>

<sup>1</sup>School of Biological Sciences, Seoul National University, Seoul 08826, Korea, <sup>2</sup>Computational Biology & Genomics, Biogen, Cambridge, MA 02142, USA, <sup>3</sup>These authors contributed equally to this work.

\*Correspondence: [depark@snu.ac.kr](mailto:depark@snu.ac.kr)

<https://doi.org/10.14348/molcells.2019.0140>

[www.molcells.org](http://www.molcells.org)

**$\beta$ Pix is a guanine nucleotide exchange factor for the Rho family small GTPases, Rac1 and Cdc42. It is known to regulate focal adhesion dynamics and cell migration. However, the *in vivo* role of  $\beta$ Pix is currently not well understood. Here, we report the production and characterization of  $\beta$ Pix-KO mice. Loss of  $\beta$ Pix results in embryonic lethality accompanied by abnormal developmental features, such as incomplete neural tube closure, impaired axial rotation, and failure of allantois-chorion fusion. We also generated  $\beta$ Pix-KO mouse embryonic fibroblasts (MEFs) to examine  $\beta$ Pix function in mouse fibroblasts.  $\beta$ Pix-KO MEFs exhibit decreased Rac1 activity, and defects in cell spreading and platelet-derived growth factor (PDGF)-induced ruffle formation and chemotaxis. The average size of focal adhesions is increased in  $\beta$ Pix-KO MEFs. Interestingly,  $\beta$ Pix-KO MEFs showed increased motility in random migration and rapid wound healing with elevated levels of MLC2 phosphorylation. Taken together, our data demonstrate that  $\beta$ Pix plays essential roles in early embryonic development, cell spreading, and cell migration in fibroblasts.**

**Keywords:**  $\beta$ Pix, cell motility, embryonic lethality, focal adhesion, mouse embryonic fibroblast

## INTRODUCTION

Cytoskeletal rearrangement is a fundamental step in the regulation of numerous cellular responses, such as proliferation, differentiation, and movement. Rho-family small GTPases, including Rac1, Cdc42, and Rho, are potent determinants that modulate actin cytoskeleton organization by cycling between an active GTP-bound state and an inactive GDP-bound state (Etienne-Manneville and Hall, 2002). Among regulatory proteins of Rho GTPases activity, guanine nucleotide exchange factors (GEFs) activate the GTPases by enhancing the exchange of bound GDP for GTP (Bos et al., 2007).

$\beta$ Pix (beta-PAK [p21-activated kinase] interacting exchange factor) is a member of the Dbl family of GEFs, containing DH and PH domains (Zheng, 2001).  $\beta$ Pix was firstly identified as a protein localized in focal adhesions (Oh et al., 1997), and it was later shown to act as a GEF for Rac1 and Cdc42 (Koh et al., 2001). Through its GEF activity,  $\beta$ Pix modulates diverse cellular events, such as remodeling of the actin cytoskeleton, platelet-derived growth factor (PDGF)-stimulated response, and cell migration (Campa et al., 2006; Kim et al., 2001; ten Klooster et al., 2006). Therefore, investigating the molecular mechanism of  $\beta$ Pix in these processes and examining the effect of disrupting  $\beta$ Pix expression in animal models are essen-

Received 24 June, 2019; revised 11 July, 2019; accepted 12 July, 2019; published online 9 August, 2019

eISSN: 0219-1032

©The Korean Society for Molecular and Cellular Biology. All rights reserved.

©This is an open-access article distributed under the terms of the Creative Commons Attribution-NonCommercial-ShareAlike 3.0 Unported License. To view a copy of this license, visit <http://creativecommons.org/licenses/by-nc-sa/3.0/>.

tial for understanding the function of  $\beta$ Pix *in vivo*.

Previous studies on the role of  $\beta$ Pix were mainly carried out using *in vitro* cell culture systems while  $\beta$ Pix genetic manipulation was carried out in model organisms, including *Caenorhabditis elegans* (Martin et al., 2016) and zebrafish (Liu et al., 2007; Tay et al., 2010). Here, we report the generation of  $\beta$ Pix-knockout ( $\beta$ Pix-KO) mice through gene targeting. These mice were used for investigating the physiological roles of  $\beta$ Pix *in vivo*. Additionally, we generated  $\beta$ Pix-KO mouse embryonic fibroblasts (MEFs) from the  $\beta$ Pix-KO embryos to investigate the role of  $\beta$ Pix at the cellular level.

In this study, we found that loss of  $\beta$ Pix causes defects in early embryonic development that lead to embryonic lethality at embryonic day 9.5 (E9.5).  $\beta$ Pix-KO MEFs have defects in cell spreading, PDGF-induced ruffle formation and chemotaxis, and focal adhesion formation. Taken together, our research suggests that  $\beta$ Pix plays essential roles in early embryonic development, cell spreading, and cell migration in fibroblasts.

## MATERIALS AND METHODS

### Generation of $\beta$ Pix-KO mice

Genomic fragment of mouse *ARHGEF7* gene was cloned by screening a CITB mouse BAC clone library (Invitrogen, USA). To generate a gene-targeting vector for *ARHGEF7*, a 3.1 kb and a 3.4 kb fragments flanking the exon 19 of this gene were cloned into Os.Dup/Del vector respectively, which carries a neomycin-resistance ( $\text{Neo}^R$ ) cassette that replaces the exon 19 and a thymidine kinase cassettes. J-1 ES cells were maintained, electroporated with the targeting vector and neomycin-selected. Survived clones were analyzed for proper recombination after digestion with either EcoRI or SacI. Targeted ES cells were microinjected into the blastocysts of C57BL/6J mice. Resulting founders were mated with C57BL/6J mice (Charles River Laboratories, USA) and germ line transmission was confirmed by Southern blotting and polymerase chain reaction of genomic DNA. For generation of  $\beta$ Pix-KO mice, interbreeding of  $\beta$ Pix-heterozygous ( $\beta$ Pix-HET) mice was performed. All mice were bred and kept in specific pathogen-free animal facilities at Seoul National University and the committees on Animal Research at Seoul National University (approval No. SNU-160321-2-5) approved all procedures.

### Antibodies and reagents

Rabbit polyclonal antibodies against the SH3 domain of  $\beta$ Pix were prepared as described previously (Oh et al., 1997). The following antibodies were purchased: monoclonal mouse antibody against Actin (clone AC-40; Sigma, USA), monoclonal mouse antibody against Git1 (clone 13/p95PKL; BD Transduction Laboratories, USA), polyclonal rabbit antibody against PAK1 (Santa Cruz Biotechnology, USA), polyclonal rabbit antibody against phospho-PAK1 (Ser199/204)/PAK2 (Ser192/197) (Cell Signaling, USA), monoclonal mouse antibody against Rac1 (clone 23A8; Millipore, USA), monoclonal mouse antibody against phospho-MLC2 (Ser19) (Cell Signaling), polyclonal rabbit antibody against phospho-MLC2 (Thr18/Ser19) (Cell Signaling), monoclonal mouse antibody

against Vinculin (clone hVIN-1; Sigma). The following reagents were purchased: Fibronectin from bovine plasma (Sigma) and PDGF-BB human (Sigma).

### Western blot analysis

Tissue and cell lysates were prepared as described previously (Oh et al., 1997; Shin et al., 2019; Shrestha et al., 2018). Protein concentrations in the tissue and cell lysates were measured by Bradford assay and with Pierce BCA Protein Assay Reagent (Thermo Scientific, USA), respectively. Equal amounts of protein were resolved by SDS-PAGE and transferred to a PVDF membrane (Millipore). Blots were blocked with 5% skim milk or 3% bovine serum albumin in 0.1% Triton X-100 in PBS (0.1% PBS-T) for 50 min. The blots were incubated with primary antibodies for 1 h at room temperature. Then, the blots were incubated with horseradish peroxidase-conjugated secondary antibodies (Jackson ImmunoResearch Laboratories, USA) for 50 min and analyzed by enhanced chemiluminescence.  $\alpha$ -Actin was used as a loading control.

### Whole mount and histological analysis of mouse embryos

To observe the whole mounted embryos, embryos of each genotypes were dissected out. Embryos were fixed 4% paraformaldehyde (PFA) (Sigma) and observed under Zeiss Lumar V12 using a 0.8 $\times$  (NeoLumar S; Zeiss, Germany) objective lens. For histological analysis, the whole mouse deciduae was dissected out and fixed in Bouin's fixative or 4% PFA. Fixed embryos were then dehydrated and embedded in paraffin and 10  $\mu$ m sections were collected on slides. Slides were stained with hematoxylin.

### Generation and culture of $\beta$ Pix-KO and $\beta$ Pix-rescue MEFs

$\beta$ Pix-HET mice were intercrossed, and embryos at E8.5 were isolated and triturated in CellStripper non-enzymatic cell dissection solution (Mediatech, USA), then attached to culture dish. Genomic DNA from yolk sac was used for genotyping. For immortalization, cells were infected with pBabe-Puro-SV40 large T Antigen lentiviral supernatant overnight. After several days or weeks of infection, immortalized cells were cultured into single cell colonies, and finally established as wild-type (WT) and  $\beta$ Pix-KO MEF lines. To establish  $\beta$ Pix-rescue MEF lines, pCAG-Cre recombinase was transfected in  $\beta$ Pix-KO cell with LipofectAMINE<sup>PLUS</sup> (Invitrogen) according to the manufacturer's instructions to splice out  $\text{Neo}^R$  cassette. After transfection, transfected cells were cultured into single cell colonies, and  $\beta$ Pix-rescue in the cells was confirmed by genotyping and western blotting. The MEFs were cultured in DMEM (Gibco, USA) supplemented with 10% certified fetal bovine serum (Gibco), 1% MEM non-essential amino acid (Gibco), 1% L-glutamine (Welgene, Korea), 0.1%  $\beta$ -mercaptoethanol (Gibco) and 1% antibiotics/antimycotics mixture (Gibco) in 5% CO<sub>2</sub> incubator at 37°C. Coverslips or dishes was coated with 10  $\mu$ g/ml fibronectin.

### Immunocytochemistry

Cultured cells on coverslips were fixed with 3.7% PFA for 10 min, permeabilized with 0.1% Triton X-100 for 10 min and blocked with blocking solution (10% normal goat serum

[Vector Laboratories, USA], 0.3% bovine serum albumin, and 0.1% PBS-T) for 1 h. Then the coverslips were incubated with primary antibodies diluted in blocking solution for 1 h at room temperature and stained with FITC-conjugated anti-mouse IgG (Jackson ImmunoResearch Laboratories) for 1 h. For actin staining, Rhodamine-phalloidin (Molecular Probes, USA) was used. Following incubation, coverslips were mounted with Vectashield (Vector Laboratories) and observed with the Axiovert 200M microscope (Zeiss) equipped with a Zeiss AxioCam HRm CCD camera using a 100 $\times$ , 1.40 Plan-Apochromat objective lens or with a LSM700 confocal microscope (Zeiss) using a 10 $\times$ , 1.20 Plan-Apochromat objective lens.

#### Cell spreading assay

MEFs were transfected with pEGFP-C1 with Metafectene Pro (Biontex Laboratories, Germany) for 24 h, and re-plated on fibronectin-coated coverslip. After 1 h incubation, cells were fixed with 3.7% PFA, and mounted. Green fluorescent protein (GFP) signals were analyzed for calculating cell spreading area with ImageJ software.

#### Analysis of ruffle formation

MEFs were cultured on fibronectin-coated coverslip and serum starved overnight. Then treated with PDGF-BB (10 ng/ml) for 7 min, cells were fixed with 3.7% PFA and stained for actin cytoskeleton, and analyzed manually for PDGF-induced ruffle formation. The cells were categorized as peripheral ruffle-, dorsal ruffle-, and peripheral and dorsal ruffle-bearing cells (Abercrombie et al., 1970; Suetsugu et al., 2003).

#### Transwell assay

For the chemotaxis assay, Costar Transwell Permeable Support (8.0  $\mu$ m pore size; Corning, USA) was used according to manufacturer's protocol. In brief, set 6000 serum starved MEFs in upper chamber, and filled serum-free media or PDGF-BB (20  $\mu$ g/ml) containing media in lower chamber. After 4 h incubation, transwell membranes were fixed with methanol, stained with eosin, mounted with Richard-Allan Scientific Mounting Medium (Thermo Scientific) and observed with Axioimager M1 (Zeiss). Migrated cells were manually counted and analyzed.

#### Analysis of focal adhesion morphology

MEFs were cultured on fibronectin-coated coverslip for 1 h, fixed with 3.7% PFA and stained focal adhesions with Vinculin antibody. The Vinculin-staining puncta were analyzed to quantitate size and number of focal adhesions. The mean fluorescence intensity was measured in ImageJ software in a blinded manner.

#### Single cell migration assay

MEFs were cultured on fibronectin-coated 35 mm dish for 4 h, and observed in a heated chamber at 37°C. Images were taken every 10 min over 4 h using the Axiovert 200M microscope, and cell migration was analyzed using ImageJ mTrackJ plugin.

#### Wound healing assay

Confluent MEFs were cultured on fibronectin-coated 35 mm dish for 4 h, then scratched with a pipette tip. Immediately after wounding, cultures were fed with fresh medium supplemented 0.1% fetal bovine serum and observed in a heated chamber at 37°C. Images were taken every 30 min over 12 h using the Axiovert 200M microscope and the wounded area was measured using ImageJ software.

#### GST-PBD pull-down assays

For GST-PBD pull-down assay, MEFs were processed as detailed elsewhere (Benard and Bokoch, 2002). In brief, cells were plated on fibronectin-coated 100 mm dish for 24 h. Then, the cells were lysed in pull-down buffer (50 mM HEPES, pH 7.4, 150 mM NaCl, 15 mM NaF, 1 mM Na<sub>3</sub>VO<sub>4</sub>, 0.5% NP-40, 1  $\mu$ g/ml leupeptin, 1  $\mu$ g/ml aprotinin, and 1  $\mu$ g/ml pepstatin), and centrifuged for 15 min at 22,250g in 4°C. The supernatant was incubated with 5  $\mu$ g of purified GST-PBD proteins pre-bound to Glutathione Sepharose 4B for 1 h at 4°C, and washed with pull-down buffer three times to remove unbound proteins. Then, the bound proteins were subjected to SDS-PAGE and western blotting.

#### Statistics

All data were expressed as mean  $\pm$  standard error of the mean. Statistical significances for measurements were calculated using Student's *t*-tests and defined as \**P* < 0.05, \*\**P* < 0.01, and \*\*\**P* < 0.001.

## RESULTS

### Loss of $\beta$ Pix results in embryonic lethality at E9.5

$\beta$ Pix-HET mice were established (Fig. 1A), and intercrossed to generate homozygous  $\beta$ Pix-KO mice. Genotyping of the pups revealed that no homozygous  $\beta$ Pix-KO mice were born, and only WT and  $\beta$ Pix-HET mice were present in the littermates at an approximately 1:2 ratio. This result indicated that total deletion of  $\beta$ Pix resulted in embryonic lethality. To identify when embryonic lethality occurs, the pregnant female mice at different gestation days were sacrificed and the embryos were examined. We found growth-retarded  $\beta$ Pix-KO embryos between E8.5 and E9.5, and resorption of these embryos at E10.  $\beta$ Pix-KO embryos at E8.5 showed complete lack of  $\beta$ Pix expression (Fig. 1B). The expression levels of Rac1 and PAK1, which are binding partners of  $\beta$ Pix (Koh et al., 2001), were not affected, but the levels of active PAK1, detected by p-PAK1 antibody (Chong et al., 2001), and Git1 were reduced in  $\beta$ Pix-KO embryos (Fig. 1B), indicating that  $\beta$ Pix deficiency can affect the activity of PAK1 and the expression level of Git1.

To investigate the morphological phenotype of  $\beta$ Pix-KO embryos, E9.5 embryos were dissected from the decidua and their gross appearances were observed under a stereomicroscope.  $\beta$ Pix-KO embryos were smaller in size than WT embryos, indicating growth retardation with developmental delays (Fig. 1C). Most  $\beta$ Pix-KO embryos exhibited impaired axial rotation and incomplete closure of the neural tube from the hindbrain to the forebrain (Figs. 1C and 1E). Another striking feature was the failure of allantois-chorion fusion (Figs. 1D

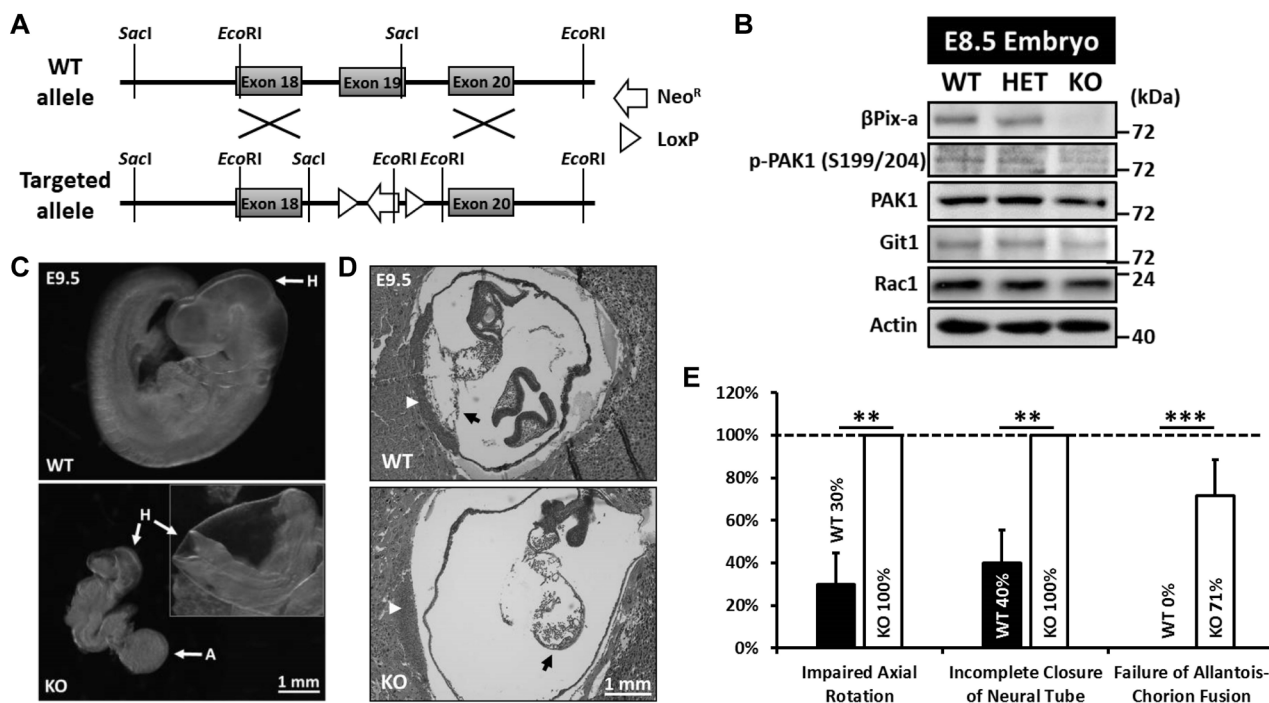


**Fig. 1. Loss of  $\beta$ Pix results in embryonic lethality at E9.5.** (A) Gene targeting strategy for generation of  $\beta$ Pix-KO mice. The exon 19 is replaced by Neo<sup>R</sup> cassette between LoxP sites. (B) Representative blots for  $\beta$ Pix-related proteins. Equal amounts of 5  $\mu$ g homogenates were loaded per lane. Antibodies used for the blots are shown at the left. (C) Representative images for whole mount analysis of E9.5 embryos. H, head; A, allantois. (D) Representative images for histological analysis of E9.5 embryos in deciduae. Black arrows indicate allantois and white arrowheads indicate chorion. (E) Quantification of the defects in axial rotation, neural tube closure and allantois-chorion fusion. Embryos (9-11) were analyzed in each group. \*\* $P < 0.01$ , \*\*\* $P < 0.001$ .

and 1E). The allantois of the  $\beta$ Pix-KO embryo was unattached to the chorion and resembled balloon-shaped debris (Fig. 1D). Taken together, this demonstrates that  $\beta$ Pix plays essential roles in early embryonic development.

### $\beta$ Pix-KO MEFs show defects in cell spreading, and PDGF-induced ruffle formation and chemotaxis

$\beta$ Pix-KO MEFs were generated from E8.5 embryos prior to embryonic lethality.  $\beta$ Pix-KO MEFs show no expression of  $\beta$ Pix, while  $\beta$ Pix-rescue MEFs show recovery of  $\beta$ Pix expression (Fig. 2A). Given that  $\beta$ Pix is a well-known activator of Rac1, we measured the levels of activated Rac1 in the MEFs using GST-PBD pull-down assay.  $\beta$ Pix-KO MEFs exhibited decreased levels of Rac1 activation compared to WT MEFs, while  $\beta$ Pix-rescue MEFs showed recovery of Rac1 activation (Fig. 2B).

Previously, it was shown that cell spreading on fibronectin is decreased upon knockdown of  $\beta$ Pix expression (ten Klooster et al., 2006). Therefore, we investigated the cell spreading of  $\beta$ Pix-KO MEFs on fibronectin (Figs. 2C and 2D). The spread area of  $\beta$ Pix-KO MEFs decreased by 34% to 37% compared with that of WT MEFs, and  $\beta$ Pix-rescue MEFs effectively recovered cell spreading ability (Fig. 2D). These results demonstrate that  $\beta$ Pix is important for cell spreading on fibronectin.

$\beta$ Pix and Rac1 play pivotal roles in PDGF responses, including ruffle formation and chemotaxis (Campa et al., 2006). To investigate the effects of  $\beta$ Pix deficiency on PDGF-induced

ruffle formation, we examined peripheral and dorsal ruffles in the MEFs upon PDGF treatment. Peripheral and dorsal ruffles were found in 40.2% and 13.6% of the WT MEFs, respectively (Fig. 2E). However, in  $\beta$ Pix-KO MEFs, the peripheral ruffle-forming cell population decreased by 25% to 54% and the dorsal ruffle-forming cell population decreased by 79% to 93%. Dorsal ruffle formation was more drastically affected by  $\beta$ Pix deficiency than peripheral ruffle formation. Additionally, cells bearing both peripheral and dorsal ruffles were also dramatically decreased in  $\beta$ Pix-KO MEFs.  $\beta$ Pix-rescue MEFs effectively recovered the ruffle-forming abilities. Next, we examined PDGF-induced chemotaxis of  $\beta$ Pix-KO MEFs using a transwell assay. Migration of WT MEFs was increased 1.42 fold in response to PDGF (Fig. 2F). However, this increase was not found in  $\beta$ Pix-KO MEFs. PDGF-induced chemotaxis was recovered to WT levels in  $\beta$ Pix-rescue MEFs. These data indicate that  $\beta$ Pix plays critical roles in ruffle formation and chemotaxis in response to PDGF in fibroblasts.

### $\beta$ Pix-KO MEFs have larger focal adhesions and increased random cell motility

$\beta$ Pix is known to regulate focal adhesion (Rosenberger and Kutsche, 2006). To examine the effects of  $\beta$ Pix deficiency on focal adhesion, focal adhesions in the MEFs were visualized with Vinculin staining, and the size of the focal adhesion was measured (Fig. 3A). In  $\beta$ Pix-KO MEFs, the average size of focal adhesion was approximately 30% larger than that in



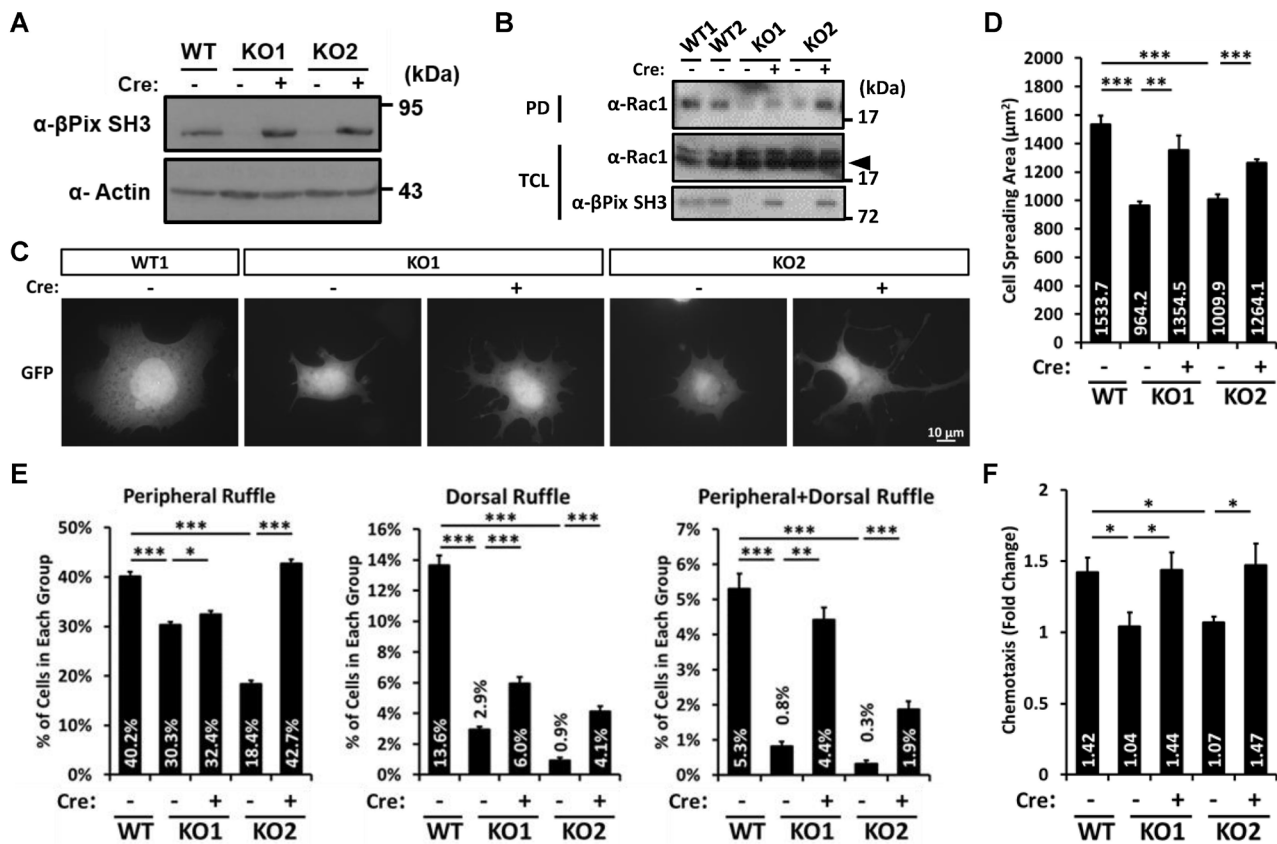


**Fig. 2.  $\beta$ Pix-KO MEF shows defects in cell spreading, and PDGF-induced ruffle formation and chemotaxis.** (A) Expression of  $\beta$ Pix protein in WT,  $\beta$ Pix-KO MEFs (KO1 and KO2 without Cre), and  $\beta$ Pix-rescue MEFs (KO1 and KO2 with Cre). Equal amounts of 12  $\mu$ g lysates were loaded per lane. (B) Active Rac1 level determined by GST-PBD pull-down assay. PD, pull-down; TCL, total cell lysate. (C and D) Representative images for the MEFs transfected with GFP (C) and quantification of cell spreading area (D). At least 100 cells from 4 independent experiments were analyzed in each group. (E) Ruffle formation in response to PDGF in the MEFs. Cells (2698-5697) from 4 independent experiments were analyzed in each group. (F) Chemotaxis in response to PDGF. The number of migratory cells was counted in 134-268 random fields from 7 independent experiments in each group. \* $P < 0.05$ , \*\* $P < 0.01$ , \*\*\* $P < 0.001$ .

WT MEFs, and this increase was reduced in  $\beta$ Pix-rescue MEFs (Fig. 3B). These results showed that  $\beta$ Pix plays a critical role in the regulation of focal adhesion in fibroblasts. The turnover of focal adhesions is highly coordinated and important for adhesion-dependent processes, such as cell migration (Raftopoulos and Hall, 2004). It was reported that reduced expression of  $\beta$ Pix by RNA interference resulted in defects in cell migration (Hua et al., 2011; Kuo et al., 2011; Sero and Bakal, 2017). Interestingly, in a single cell motility assay, the total migrated distance of  $\beta$ Pix-KO MEFs was increased when compared with that of WT MEFs and this increase was reduced in  $\beta$ Pix-rescue MEFs (Fig. 3C). Likewise, in a wound healing assay (Fig. 3D), the rate of wound closure was increased in  $\beta$ Pix-KO MEFs compared with that of WT MEFs and this increase was reduced in  $\beta$ Pix-rescue MEFs (Fig. 3E). These data indicate that a deficiency of  $\beta$ Pix induces an increase in cell motility in the MEFs.

#### $\beta$ Pix-KO MEFs showed enhanced Ser19 phosphorylation of MLC2

A recent study showed that  $\beta$ Pix knockdown promotes kera-

tinocyte motility via myosin light chain activation (Hiroyasu et al., 2017). Given that  $\beta$ Pix-KO MEFs have increased motility (Figs. 3C-3E), we investigated the level of MLC2 activation by measuring the Ser19 phosphorylation of MLC2 which is commonly used as an index for MLC2 activation (Amano et al., 1996).  $\beta$ Pix-KO MEFs showed increased levels of MLC2 phosphorylation, with this increase reduced in  $\beta$ Pix-rescue MEFs (Figs. 4A and 4B). Likewise,  $\beta$ Pix-KO MEFs showed an increase in p-MLC2 signal by immunocytochemistry (Fig. 4C), and this increase was reduced in  $\beta$ Pix-rescue MEFs (Figs. 4C and 4D). These results suggest that  $\beta$ Pix deficiency may induce MLC2 activation, thus increasing actomyosin contractility to enhance cell motility.

## DISCUSSION

### $\beta$ Pix deficiency results in early embryonic lethality

A recent report from Omelchenko et al. (2014) showed that  $\beta$ Pix-KO embryos have defects in the collective cell migration of anterior visceral endoderm cells. The defects, such as incomplete closure of the neural tube and impaired axial

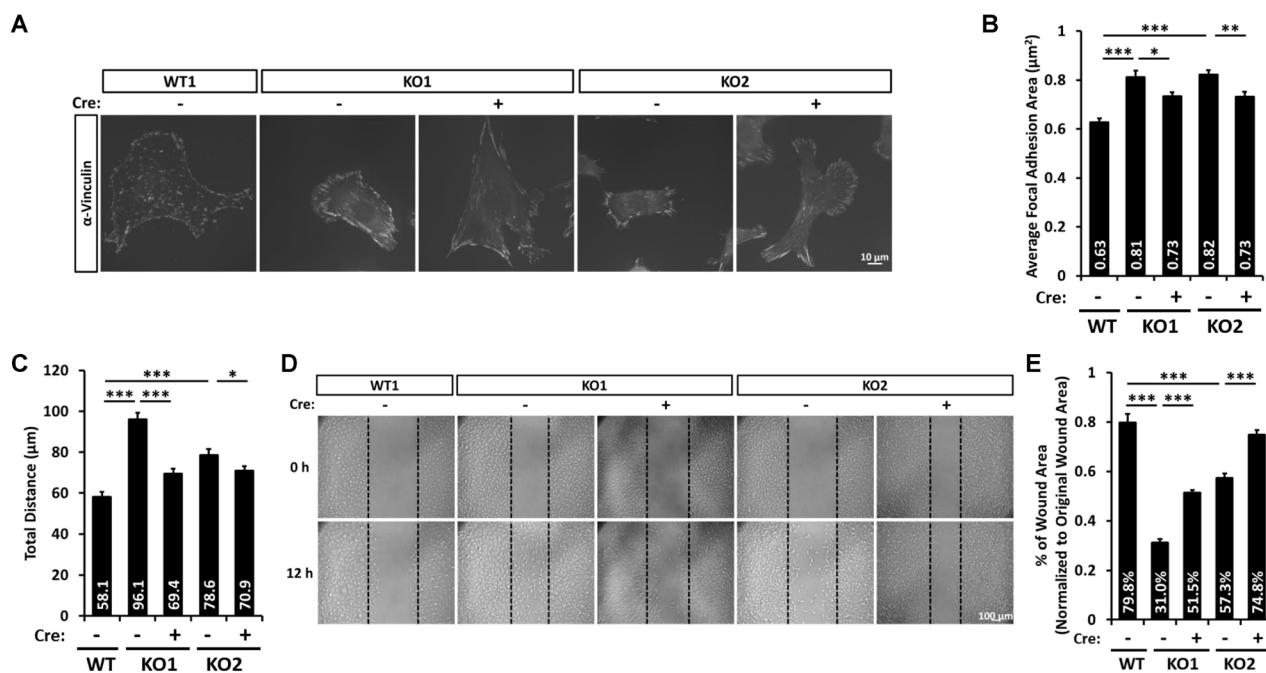


**Fig. 3.  $\beta$ Pix-KO MEFs have increase in focal adhesion size and cell motility.** (A and B) Representative images for focal adhesions visualized by Vinculin-staining (A) and average focal adhesion area (B) in the MEFs. Cells (65-106) from 5 independent experiments were analyzed per group. (C) Total migrated distance of the MEFs in single cell migration assay. At least 53 cells from 3 independent experiments were analyzed in each group. (D) Representative images of wound healing assay for the MEFs. Two dotted lines indicate original boundary lines of scratch. (E) Ratio of wound area for 12 h to 0 h after wound generation is shown. Four experiments were analyzed in each group. \* $P < 0.05$ , \*\* $P < 0.01$ , \*\*\* $P < 0.001$ .

rotation (Figs. 1C and 1E), may be caused by this abnormal collective cell migration.  $\beta$ Pix deficiency also shows failure of allantois-chorion fusion (Figs. 1D and 1E). Allantois-chorion fusion largely relies on the interaction between  $\alpha 4$  integrin in the chorion and VCAM1 of the allantois (Kwee et al., 1995; Yang et al., 1995). Genomic ablation of  $\alpha 4$  integrin or VCAM1 resulted in phenotypes similar to the  $\beta$ Pix-KO embryo, in which early placental formation fails. Abi1 deficient mice also show embryonic lethality and failure of placental development (Ring et al., 2011). Abi1 can directly interact with the  $\alpha 4$  integrin cytoplasmic tail and is important for integrin  $\alpha 4$  cellular signaling. It has also been reported that Abi1 and  $\beta$ Pix can directly interact (Campa et al., 2006). Git1, a stable interacting partner of  $\beta$ Pix, is also involved in  $\alpha 4$  integrin signaling. Git1-paxillin-integrin  $\alpha 4$  interaction is required for Rac activation at the leading edge of migrating cells (Nishiya et al., 2005).  $\beta$ Pix may play a role in the  $\alpha 4$  integrin-VCAM signaling pathway through Abi1 or Git1 to regulate placental development. Thus,  $\beta$ Pix deficiency may distort the early placental development resulting in embryonic lethality.

#### $\beta$ Pix-KO MEF cells show an increased migration distance in cell migration assay

$\beta$ Pix-KO MEFs have defects in cell spreading, and PDGF-induced ruffle formation and chemotaxis (Figs. 2C-2F). These findings suggest that  $\beta$ Pix plays essential roles in cell migra-

tion. However, unexpectedly,  $\beta$ Pix-KO MEF cells showed increased motility in both single cell migration and wound healing assays (Figs. 3C-3E). Although most studies using  $\beta$ Pix knockdown cells reported decreased motility in migration assays (Hua et al., 2011; Kuo et al., 2011; Sero and Bakal, 2017), a recent study showed that  $\beta$ Pix knockdown promotes keratinocyte motility (Hiroyasu et al., 2017). They observed no difference in activated Rac1 levels and p-MLC protein levels, but p-MLC localization was altered and traction force was increased in  $\beta$ Pix knockdown keratinocytes. They suggested that this promotion of cell motility was due to an increase in the traction force generated by enhanced actomyosin contraction, and fine tuning of spatial MLC activity is important. They also showed an increase in the size of focal adhesions in  $\beta$ Pix knockdown keratinocytes. Similar phenotypes were observed in  $\beta$ Pix-KO MEFs (Figs. 3A and 3B). Unlike  $\beta$ Pix knockdown keratinocytes,  $\beta$ Pix-KO MEFs exhibited elevated protein levels of p-MLC2 (Fig. 4). PAK family members can directly regulate phosphorylation of MLC through inhibition of the myosin light chain kinase (Sanders et al., 1999). Since  $\beta$ Pix is a positive regulator for PAK activity (Koh et al., 2001),  $\beta$ Pix-KO MEFs may induce elevated levels of p-MLC2 by repressing the inhibitory role of PAK on MLC2 phosphorylation.

In conclusion, loss of  $\beta$ Pix leads to early embryonic lethality in mice, and  $\beta$ Pix-KO MEFs exhibit defects in cell spreading, and PDGF-induced ruffle formation and chemotaxis. Interest-

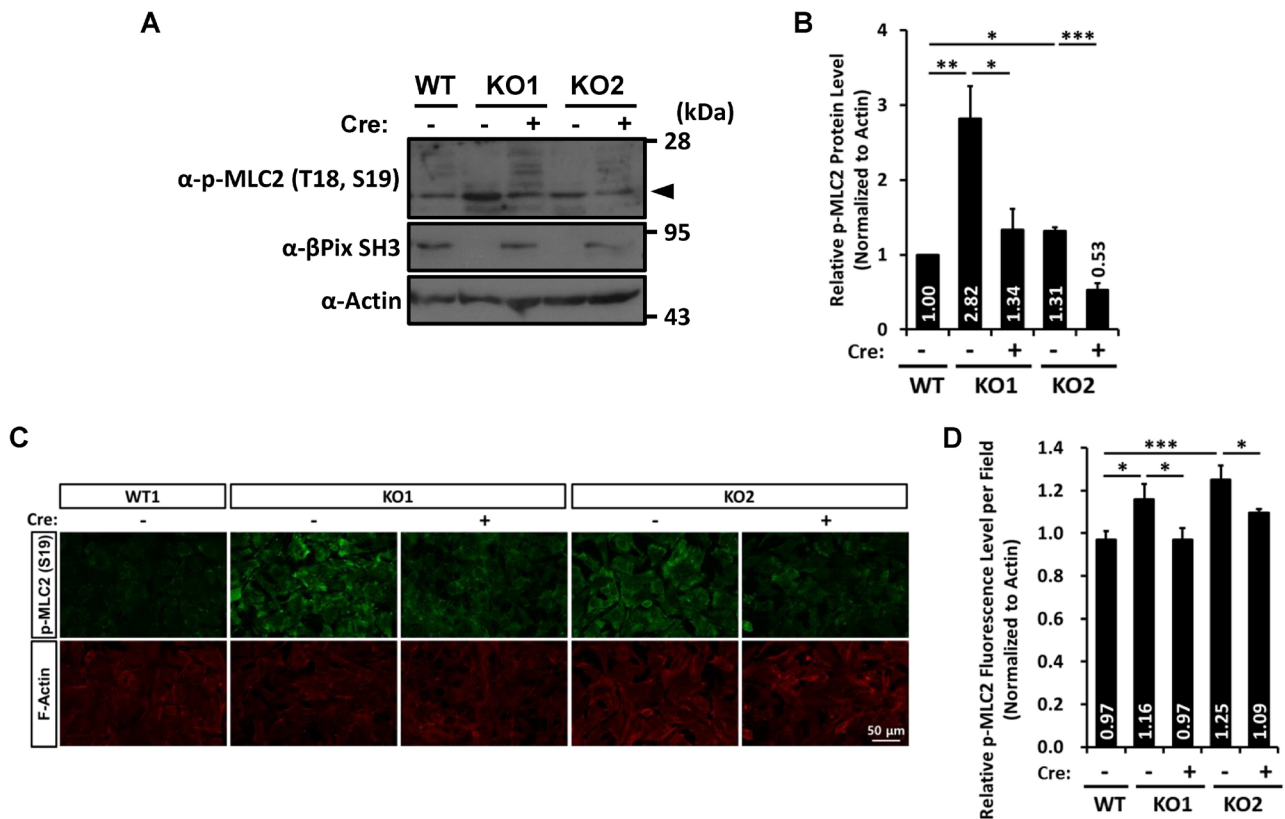


**Fig. 4.  $\beta$ Pix deficiency enhances the Ser19 phosphorylation of MLC2.** (A) Representative western blots for phosphorylated MLC2 (p-MLC2) in the MEFs. (B) Quantification of relative p-MLC2 level is shown. Four experiments were analyzed in each group. (C) Representative images for p-MLC2 in the MEFs. (D) Quantification of relative p-MLC2 level is shown. Five experiments were analyzed in each group. \* $P < 0.05$ , \*\* $P < 0.01$ , \*\*\* $P < 0.001$ .

ingly,  $\beta$ Pix-KO MEFs showed increased cell motility in single cell migration and wound healing assays, probably via inducing MLC2 activation. Detailed studies will further highlight the underlying roles of  $\beta$ Pix in embryonic development and cell migration.  $\beta$ Pix-KO MEFs will be a valuable tool for dissecting the functions of  $\beta$ Pix in diverse cellular processes.

#### Disclosure

The authors have no potential conflicts of interest to disclose.

#### ACKNOWLEDGMENTS

We thank Dr. Heiner Westphal and Alex Grinberg, who were former members in Mammalian Genes and Development, Eunice Kennedy Shriver National Institute of Child Health and Human Development, National Institutes of Health, Bethesda, USA, for advising and technical assistance for generating  $\beta$ Pix-KO mice. This work was supported by the Basic Science Research Program through the National Research Foundation of Korea (NRF-2016R1D1A1B03934362 and NRF-2017R1A2B4006259).

#### ORCID

Taeln Kang <https://orcid.org/0000-0001-9662-865X>  
 Seung Joon Lee <https://orcid.org/0000-0001-6690-2830>  
 Younghee Kwon <https://orcid.org/0000-0003-2747-2502>  
 Dongeun Park <https://orcid.org/0000-0003-2010-4598>

#### REFERENCES

- Abercrombie, M., Heaysman, J.E., and Pegrum, S.M. (1970). The locomotion of fibroblasts in culture. II. "RRuffling". *Exp. Cell Res.* 60, 437-444.
- Amano, M., Ito, M., Kimura, K., Fukata, Y., Chihara, K., Nakano, T., Matsuura, Y., and Kaibuchi, K. (1996). Phosphorylation and activation of myosin by Rho-associated kinase (Rho-kinase). *J. Biol. Chem.* 271, 20246-20249.
- Benard, V. and Bokoch, G.M. (2002). Assay of Cdc42, Rac, and Rho GTPase activation by affinity methods. *Methods Enzymol.* 345, 349-359.
- Bos, J.L., Rehmann, H., and Wittinghofer, A. (2007). GEFs and GAPs: critical elements in the control of small G proteins. *Cell* 129, 865-877.
- Campa, F., Machuy, N., Klein, A., and Rudel, T. (2006). A new interaction between Abi-1 and betaPIX involved in PDGF-activated actin cytoskeleton reorganization. *Cell Res.* 16, 759-770.
- Chong, C., Tan, L., Lim, L., and Manser, E. (2001). The mechanism of PAK activation. Autophosphorylation events in both regulatory and kinase domains control activity. *J. Biol. Chem.* 276, 17347-17353.
- Etienne-Manneville, S. and Hall, A. (2002). Rho GTPases in cell biology. *Nature* 420, 629-635.
- Hiroyasu, S., Stimac, G.P., Hopkinson, S.B., and Jones, J.C.R. (2017). Loss of beta-PIX inhibits focal adhesion disassembly and promotes keratinocyte motility via myosin light chain activation. *J. Cell Sci.* 130, 2329-2343.
- Hua, K.T., Tan, C.T., Johansson, G., Lee, J.M., Yang, P.W., Lu, H.Y., Chen, C.K., Su, J.L., Chen, P.B., Wu, Y.L., et al. (2011). N-alpha-acetyltransferase 10 protein suppresses cancer cell metastasis by binding PIX proteins and

inhibiting Cdc42/Rac1 activity. *Cancer Cell* 19, 218-231.

Kim, S., Lee, S.H., and Park, D. (2001). Leucine zipper-mediated homodimerization of the p21-activated kinase-interacting factor, beta Pix. Implication for a role in cytoskeletal reorganization. *J. Biol. Chem.* 276, 10581-10584.

Koh, C.G., Manser, E., Zhao, Z.S., Ng, C.P., and Lim, L. (2001). Beta1PIX, the PAK-interacting exchange factor, requires localization via a coiled-coil region to promote microvillus-like structures and membrane ruffles. *J. Cell Sci.* 114, 4239-4251.

Kuo, J.C., Han, X., Hsiao, C.T., Yates, J.R., 3rd, and Waterman, C.M. (2011). Analysis of the myosin-II-responsive focal adhesion proteome reveals a role for beta-Pix in negative regulation of focal adhesion maturation. *Nat. Cell Biol.* 13, 383-393.

Kwee, L., Baldwin, H.S., Shen, H.M., Stewart, C.L., Buck, C., Buck, C.A., and Labow, M.A. (1995). Defective development of the embryonic and extraembryonic circulatory systems in vascular cell adhesion molecule (VCAM-1) deficient mice. *Development* 121, 489-503.

Liu, J., Fraser, S.D., Faloon, P.W., Rollins, E.L., Vom Berg, J., Starovic-Subota, O., Laliberte, A.L., Chen, J.N., Serluca, F.C., and Childs, S.J. (2007). A betaPix Pak2a signaling pathway regulates cerebral vascular stability in zebrafish. *Proc. Natl. Acad. Sci. U. S. A.* 104, 13990-13995.

Martin, E., Ouellette, M.H., and Jenna, S. (2016). Rac1/RhoA antagonism defines cell-to-cell heterogeneity during epidermal morphogenesis in nematodes. *J. Cell Biol.* 215, 483-498.

Nishiya, N., Kiosses, W.B., Han, J., and Ginsberg, M.H. (2005). An alpha4 integrin-paxillin-Arf-GAP complex restricts Rac activation to the leading edge of migrating cells. *Nat. Cell Biol.* 7, 343-352.

Oh, W.K., Yoo, J.C., Jo, D., Song, Y.H., Kim, M.G., and Park, D. (1997). Cloning of a SH3 domain-containing proline-rich protein, p85SPR, and its localization in focal adhesion. *Biochem. Biophys. Res. Commun.* 235, 794-798.

Omelchenko, T., Rabadan, M.A., Hernandez-Martinez, R., Grego-Bessa, J., Anderson, K.V., and Hall, A. (2014).  $\beta$ -Pix directs collective migration of anterior visceral endoderm cells in the early mouse embryo. *Genes Dev.* 28, 2764-2777.

Raftopoulou, M. and Hall, A. (2004). Cell migration: Rho GTPases lead the way. *Dev. Biol.* 265, 23-32.

Ring, C., Ginsberg, M.H., Haling, J., and Pendergast, A.M. (2011). Abl-interactor-1 (Abi1) has a role in cardiovascular and placental development and is a binding partner of the alpha4 integrin. *Proc. Natl. Acad. Sci. U. S. A.* 108, 149-154.

Rosenberger, G. and Kutsche, K. (2006). AlphaPIX and betaPIX and their role in focal adhesion formation. *Eur. J. Cell Biol.* 85, 265-274.

Sanders, L.C., Matsumura, F., Bokoch, G.M., and de Lanerolle, P. (1999). Inhibition of myosin light chain kinase by p21-activated kinase. *Science* 283, 2083-2085.

Sero, J.E. and Bakal, C. (2017). Multiparametric analysis of cell shape demonstrates that beta-PIX directly couples YAP activation to extracellular matrix adhesion. *Cell Syst.* 4, 84-96.e6.

Shin, M.S., Song, S.H., Shin, J.E., Lee, S.H., Huh, S.O., and Park, D. (2019). Src-mediated phosphorylation of betaPix-b regulates dendritic spine morphogenesis. *J. Cell Sci.* 132, pii: jcs224980.

Shrestha, D., Choi, D., and Song, K. (2018). Actin dysfunction induces cell cycle delay at G2/M with sustained ERK and RSK activation in IMR-90 normal human fibroblasts. *Mol. Cells* 41, 436-443.

Suetsugu, S., Yamazaki, D., Kurisu, S., and Takenawa, T. (2003). Differential roles of WAVE1 and WAVE2 in dorsal and peripheral ruffle formation for fibroblast cell migration. *Dev. Cell* 5, 595-609.

Tay, H.G., Ng, Y.W., and Manser, E. (2010). A vertebrate-specific Chp-PAK-PIX pathway maintains E-cadherin at adherens junctions during zebrafish epiboly. *PLoS One* 5, e10125.

ten Klooster, J.P., Jaffer, Z.M., Chernoff, J., and Hordijk, P.L. (2006). Targeting and activation of Rac1 are mediated by the exchange factor beta-Pix. *J. Cell Biol.* 172, 759-769.

Yang, J.T., Rayburn, H., and Hynes, R.O. (1995). Cell adhesion events mediated by alpha 4 integrins are essential in placental and cardiac development. *Development* 121, 549-560.

Zheng, Y. (2001). Dbl family guanine nucleotide exchange factors. *Trends Biochem. Sci.* 26, 724-732.